Letter | Editors' Suggestion

Subleading conformal dimensions at the O(4) Wilson-Fisher fixed point

Debasish Banerjee[1] and Shailesh Chandrasekharan[2]

[1]*Saha Institute of Nuclear Physics, Bidhan Nagar, Kolkata, West Bengal 700064, India*
[2]*Department of Physics, Duke University, Box 90305, Durham, North Carolina 27708, USA*

(Received 6 December 2021; accepted 8 February 2022; published 25 February 2022)

In this work we focus on computing the conformal dimensions $D(j_L, j_R)$ of local fields that transform in an irreducible representation of $SU(2) \times SU(2)$ labeled with (j_L, j_R) at the $O(4)$ Wilson-Fisher fixed point using the Monte Carlo method. In the large charge expansion, among the sectors with a fixed large value of $j = \max(j_L, j_R)$, the leading sector has $|j_L - j_R| = 0$ and the subleading one has $|j_L - j_R| = 1$. Since Monte Carlo calculations at large j become challenging in the traditional lattice formulation of the $O(4)$ model, a qubit regularized $O(4)$ lattice model was used recently to compute $D(j, j)$. Here we extend those calculations to the subleading sector. Our Monte Carlo results in the range $2 \le j \le 20$ fit well to the expected large j expansion $D(j, j-1) - D(j, j) \sim \lambda_0 + \lambda_{1/2}/\sqrt{j} + \lambda_1/j + \lambda_{3/2}/j^{3/2}$, but we have to assume that at least one of the purely quantum mechanical contributions λ_0 or λ_1 is nonzero. Assuming $\lambda_0 = 0$ as conjectured recently, we find $\lambda_{1/2} \approx 2.1(1)$, $\lambda_1 \approx 2.3(2)$, and $\lambda_{3/2} \approx 1.2(2)$.

DOI: 10.1103/PhysRevD.105.L031507

I. INTRODUCTION

There has been a resurrection of interest in conformal field theories in recent years, especially due to the success of the bootstrap approach in certain problems [1,2]. It has also become clear that conformal field theories simplify in sectors with either large spin [3] or large global charge [4]. Due to these developments the field has seen a renaissance with several new results over the past few years [5–15]. A recent review of the above progress can be found in Refs. [16,17].

An interesting quantity in conformal field theory is the conformal dimension of local fields that transform according to some representation of the symmetries of the theory. In this work we focus on global symmetries and study CFTs that emerge in three-dimensional $O(N)$ models at the Wilson-Fisher fixed point. Recent work [4] showed that in these theories the conformal dimension $D(Q)$ of local fields that transform under the representation with charge Q satisfy a large charge expansion of the form

$$D(Q) = \sqrt{\frac{Q^3}{4\pi}}\left(c_{3/2} + \frac{4\pi}{Q}c_{1/2} + \mathcal{O}(1/Q^2)\right) + c_0, \qquad (1)$$

where $c_{3/2}$ and $c_{1/2}$ are low-energy constants that need to be determined nonperturbatively, while $c_0 \approx -0.094$ can be determined analytically [18,19]. We can compute $D(Q)$ through the power law decay of the Euclidean correlation function between local source $\mathcal{O}_Q$ and sink $\bar{\mathcal{O}}_Q$ fields that transform under a specific representation of the global symmetry group with charge Q and are separated by a distance x. This correlation function is expected to decay as $|x|^{-2D_Q}$. Nonperturbative Monte Carlo calculations confirming these predictions for the case of the $O(2)$ model, where the global charges Q are represented by integers, have also been performed, and it was discovered that in this case $c_{3/2} = 1.195(10)$ and $c_{1/2} = 0.075(10)$ [20]. These calculations were later extended to the $O(4)$ model where the local fields transform in some representation of the $O(4)$ symmetry. We can classify them according to the irreducible representations of $SU_L(2) \times SU_R(2)$ labeled with charges (j_L, j_R) where $j_L, j_R = 0, 1/2, 1, 3/2, \ldots$. The leading sector [i.e., the sector with the minimum value of $D(j_L, j_R)$] is the one with $|j_L - j_R| = 0$. In this sector, if we define $j = j_L = j_R$ and $Q = 2j$, then $D(j, j)$ is also given by Eq. (1). Monte Carlo calculations give $c_{3/2} = 1.068(4)$ and $c_{1/2} = 0.083(3)$ [21], and with these two leading coefficients, Eq. (1) predicts the conformal dimensions even at $Q = 1$ within a few percent.

How well does the large charge expansion predict the conformal dimensions in the subleading sector, where $|j_L - j_R| = 1$? The first two leading coefficients of $D(j, j-1)$ in the large charge expansion are expected to be the same as $D(j, j)$ and given by Eq. (1) [22]. The coefficient c_0 has also been conjectured to be the same, but in our work we assume the possibility that it is different for reasons discussed below. This implies that

$\tilde{\Delta}(j) = D(j, j-1) - D(j, j)$ will have a large charge expansion of the form

$$\tilde{\Delta}(j) = \lambda_0 + \frac{\lambda_{1/2}}{j^{1/2}} + \frac{\lambda_1}{j} + \frac{\lambda_{3/2}}{j^{3/2}} + \mathcal{O}\left(\frac{1}{j^2}\right). \quad (2)$$

The coefficients of fractional powers of j like $\lambda_{1/2}$ and $\lambda_{3/2}$ are new Wilson coefficients, similar to $c_{3/2}$ and $c_{1/2}$ in Eq. (1), that cannot, in principle, be determined within the large charge effective field theory [22]. Their origin is essentially classical with corrections coming from quantum fluctuations. On the other hand, we also include coefficients of integer powers of j like λ_0 and λ_1, which can arise from purely quantum mechanical effects [similar to c_0 in Eq. (1)] and can, in principle, be calculable analytically [23].

The spin of the leading conformal field in the (j, j) sector is different from the $(j, j-1)$ sector. Such differences were first observed in [24] and later clarified in the context of $O(4)$ in [25,26]. Given this difference between the (j, j) and the $(j, j-1)$ sectors, it seems possible that λ_0 does not vanish. However, it has been conjectured that $\lambda_0 = 0$ since it is difficult to imagine a calculation that could distinguish between $D(j, j)$ and $D(j, j-1)$ in the large j limit [27]. What about λ_1? As far as we can tell there has been no discussion of it in the literature. In order to understand if λ_0 and λ_1 can be nonzero and to estimate $\lambda_{1/2}$ and $\lambda_{3/2}$, we design a Monte Carlo method to compute $\tilde{\Delta}(j)$ as a function of j. We fit our results in the range $1 \le j \le 20$ to the general form given in Eq. (2) and try to estimate the various λ_i's numerically.

II. QUBIT REGULARIZED O(4) MODEL

In order to construct a Monte Carlo method to compute $\tilde{\Delta}(j)$ it is useful to understand how the $SU_L(2) \times SU_R(2)$ symmetry is manifest in our lattice model, which is the same as the one used in Ref. [21]. For this purpose it is helpful to view our model as strongly coupled lattice quantum electrodynamics (QED) constructed with staggered fermions [28]. When gauge fields are integrated out exactly, the microscopic degrees of freedom are made up of bosons with fermionic constituents. These bosons naturally have a built-in hardcore interaction, and hence the Hilbert space on each lattice site is finite dimensional. Such bosonic lattice field models with a finite dimensional Hilbert space, that reproduce a continuum quantum field theory, can be referred to as a qubit regularized model of the continuum quantum field theory [29]. Other examples of qubit regularized models for studying continuum quantum field theories with $O(N)$ symmetries have been constructed recently [30,31].

The lattice action of our qubit regularized $O(4)$ model can be written using four Grassmann valued lattice fields $\psi_{1,k}, \psi_{2,k}, \bar{\psi}_{1,k}, \bar{\psi}_{2,k}$ at each lattice site $k \equiv (\mathbf{r}, \tau)$ on a cubic lattice, where we distinguish between the two-dimensional spatial coordinate $\mathbf{r}$ and the Euclidean temporal coordinate τ. The Euclidean action of our model is given by [21]

$$S(\psi, \bar{\psi}) = -\sum_{\langle k,k' \rangle} \mathrm{Tr}(M_k M_{k'}) - \frac{U}{2} \sum_k \mathrm{Det}(M_k), \quad (3)$$

where $(M_k)_{a,b} = \psi_{a,k} \bar{\psi}_{b,k}$ is a 2×2 matrix defined at each lattice site k. The symbol $\langle k, k' \rangle$ refers to neighboring sites k and k'. The partition function is defined as usual through the Grassmann integral

$$Z = \int \prod_{a,k} [d\bar{\psi}_{a,k} d\psi_{a,k}] e^{-S(\psi, \bar{\psi})}. \quad (4)$$

It is easy to verify that the action is invariant under the $SU_L(2) \times SU_R(2)$ transformations given by $M_k \to L M_k R^\dagger$ when $k \in$ even sites, and $M_k \to R M_k L^\dagger$, when $k \in$ odd sites. Here we assume L and R are 2×2 matrices, each of which is an element of the $SU(2)$ group. This means $(\psi_{1,k}, \psi_{2,k})$ on even sites and $(-i\bar{\psi}_{2,k}, i\bar{\psi}_{1,k})$ on odd sites transform as $SU_L(2)$ doublets, while they are singlets of $SU_R(2)$. The same fields on the opposite parity sites transform as $SU_R(2)$ doublets and $SU_L(2)$ singlets. When $U = 0$, the theory has an additional $U(1)$ symmetry: $\psi_{a,x} \to e^{i\theta} \psi_{a,x}$ and $\bar{\psi}_{a,x} \to e^{i\theta} \bar{\psi}_{a,x}$ for the odd sites, and $\psi_{a,x} \to e^{-i\theta} \psi_{a,x}$ and $\bar{\psi}_{a,x} \to e^{-i\theta} \bar{\psi}_{a,x}$ on the even sites. The U-term, therefore, mimics the anomalous axial symmetry of the action in quantum chromodynamics (QCD) [28]. For this reason the terms in the partition function that arise due to a nonzero value of U were referred to as instantons in the earlier work. It is known that instantons are known to break the anomalous axial symmetry in QCD. In the more recent view point of qubit regularization, the instantons can be viewed as simply the local Fock vacuum states [30].

It is possible to perform the Grassmann integrations in Eq. (4) exactly and rewrite the partition as a sum over worldline configurations of pions and instantons [28]. One then obtains $Z = \sum_{[\ell]} U^{N_I}$, where $[\ell]$ is a configuration of worldlines, which is a collection of closed oriented loops, each of which can be in one of two colors, red or green. In addition, there are isolated sites which do not belong to the worldlines and are referred to as instantons. Note that N_I is the total number of instantons in the configuration. An illustration of a worldline configuration on a two-dimensional lattice is shown in Fig. 1. In an earlier work, we solved our lattice model using this worldline approach and showed that at the critical coupling of $U_c \approx 1.655394$ we can reproduce the critical scaling of the Wilson-Fisher fixed point at long distances [21].

III. LEADING CHARGE SECTORS

Our goal is to compute the conformal dimensions $D(j_L, j_R)$ of field operators that transform in some

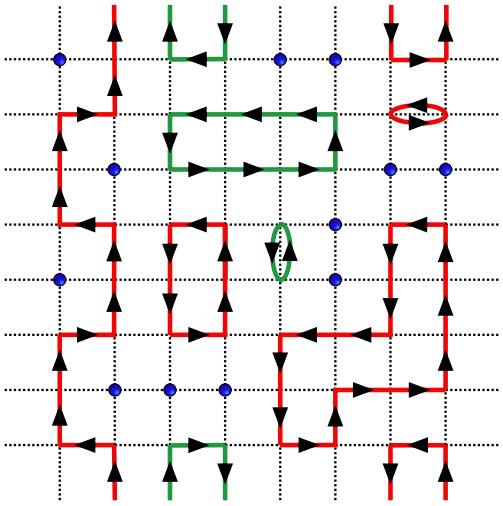

FIG. 1. Illustration of an $O(4)$ worldline configuration in $1+1$ dimensions with $N_I = 12$ instantons (blue dots). The weight of the configuration is U^{12}. Each loop is an oriented loop representing a red worldline or a green worldline.

irreducible representation (j_L, j_R) of the $SU_L(2) \times SU_R(2)$ group at the critical point. We can accomplish this by computing the correlation function

$$C_{j_L,j_R} = \langle \bar{\mathcal{O}}_{j_L,j_R} \mathcal{O}_{j_L,j_R} \rangle = \frac{1}{Z} \int \prod_{a,k} [d\bar{\psi}_{a,k} d\psi_{a,k}] e^{-S(\psi,\bar{\psi})} \bar{\mathcal{O}}_{j_L,j_R} \mathcal{O}_{j_L,j_R}, \quad (5)$$

where $\mathcal{O}_{j_L,j_R}$ and $\bar{\mathcal{O}}_{j_L,j_R}$ are the source and sink terms constructed with Grassmann valued fields that transform in the irreducible representation (j_L, j_R). In our work, the source will be located at the temporal slice $\tau = 0$, while the sink will be at the temporal slice $\tau = L/2$. Thus, at the critical point, we expect $C_{j_L,j_R} = A_{j_L,j_R} L^{-2D(j_L,j_R)}$ for sufficiently large values of L.

In order to construct $\mathcal{O}_{j_L,j_R}$ and $\bar{\mathcal{O}}_{j_L,j_R}$ that transform under the irreducible representation (j_L, j_R), let us denote $|(j_L, m_L); (j_R, m_R)\rangle$ as the $(2j_L+1)(2j_R+1)$ dimensional orthonormal basis that spans the irreducible representation space of (j_L, j_R). Here $-j_L \le m_L \le j_L$ and $-j_R \le m_R \le j_R$. We can label the fields that transform according to this irreducible representation as $\mathcal{O}_{|(j_L,m_L);(j_R,m_R)\rangle}$. For the sink terms, it is natural to choose fields that transform in the conjugate representation $\langle (j_L, m_L); (j_R, m_R)|$. We can label these sink fields as $\bar{\mathcal{O}}_{\langle (j_L,m_L);(j_R,m_R)|}$. While we can choose any of these fields as source and sink terms in the (j_L, j_R) representation, we find that choosing $m_L = j_L$ and $m_R = j_R$ will be the most convenient choice for numerical work.

Based on the transformation property of M_k it is easy to see that the four local fermion bilinear lattice fields $i\psi_{1,k}\bar{\psi}_{1,k}$, $-i\psi_{2,k}\bar{\psi}_{2,k}$, $-i\psi_{1,k}\bar{\psi}_{2,k}$, $-i\psi_{2,k}\bar{\psi}_{1,k}$ transform under the $(1/2, 1/2)$ (vector) representation of $O(4)$. However, the fields transform differently on even and odd sites. The exact mapping is given in Table I. Given the source fields we can construct the sink fields through the conjugate representation. This is given in Table II. Using the information in Tables I and II we can identify each worldline in Fig. 1 as a vector particle carrying an appropriate charge. For example, we can identify the sources and sinks of red worldlines as $\mathcal{R}_k = -i\psi_{1,k}\bar{\psi}_{2,k}$ and $\bar{\mathcal{R}}_k = -i\psi_{2,k}\bar{\psi}_{1,k}$ on all sites. On the other hand, the sources and sinks of green worldlines depend on the parity of the sites. The green source is given by $\mathcal{G}_k = i\psi_{1,k}\bar{\psi}_{1,k}$ on even sites, and $\mathcal{G}_k = -i\psi_{2,k}\bar{\psi}_{2,k}$ on odd sites. This is reversed for the sink of green lines. We have $\bar{\mathcal{G}}_k = -i\psi_{2,k}\bar{\psi}_{2,k}$ on even sites, and $\bar{\mathcal{G}}_k = i\psi_{1,k}\bar{\psi}_{1,k}$ on odd sites.

TABLE I. Local fermion bilinear fields transform according to the vector representation of $O(4)$. This table gives the explicit realization of each component at the lattice site k. As can be seen, the realization can depend on whether the site is even or odd.

Local field	Even site	Odd site
$\mathcal{O}_{\|(1/2,1/2);(1/2,1/2)\rangle}$	$-i\psi_{1,k}\bar{\psi}_{2,k}$	$-i\psi_{1,k}\bar{\psi}_{2,k}$
$\mathcal{O}_{\|(1/2,-1/2);(1/2,-1/2)\rangle}$	$i\psi_{2,k}\bar{\psi}_{1,k}$	$i\psi_{2,k}\bar{\psi}_{1,k}$
$\mathcal{O}_{\|(1/2,1/2);(1/2,-1/2)\rangle}$	$i\psi_{1,k}\bar{\psi}_{1,k}$	$-i\psi_{2,k}\bar{\psi}_{2,k}$
$\mathcal{O}_{\|(1/2,-1/2);(1/2,1/2)\rangle}$	$-i\psi_{2,k}\bar{\psi}_{2,k}$	$i\psi_{1,k}\bar{\psi}_{1,k}$

In order to construct sources of more general irreducible representations, we use the tensor product of the vector representation of local fields distributed over several spatial lattice sites on the time slice $\tau = 0$. The same sites on the time slice $\tau = L/2$ are used to construct the sinks. Let us first construct sources and sinks that transform in the representation (j, j), which we refer to as the leading sector. We know we can construct the basis state $|(j, j); (j, j)\rangle$ as a tensor product of $2j$ states of the form $|(1/2, 1/2); (1/2, 1/2)\rangle$. The source $\mathcal{O}_{|(1/2,1/2);(1/2,1/2)\rangle}$ can also be constructed in the same way, placing $2j$ local sources of red worldlines on nearby sites on a spatial lattice. In our work we choose these lattice sites k labeled as $1, 2, \ldots, 2j$ around the origin as shown in Fig. 2. Hence one of the possible sources in the (j, j) representation is then given by $\mathcal{O}_{|(j,j);(j,j)\rangle} = \mathcal{R}_1\mathcal{R}_2\ldots\mathcal{R}_{2j}$, while the corresponding sink is given by $\bar{\mathcal{O}}_{\langle (j,j);(j,j)|} = \bar{\mathcal{R}}_1\bar{\mathcal{R}}_2\ldots\bar{\mathcal{R}}_{2j}$. Here the

TABLE II. Relationship between source and sink fields on a local site.

Sink		Source
$\bar{\mathcal{O}}_{\langle (1/2,1/2);(1/2,1/2)\|}$	=	$-\mathcal{O}_{\|(1/2,-1/2);(1/2,-1/2)\rangle}$
$\bar{\mathcal{O}}_{\langle (1/2,-1/2);(1/2,-1/2)\|}$	=	$-\mathcal{O}_{\|(1/2,1/2);(1/2,1/2)\rangle}$
$\bar{\mathcal{O}}_{\langle (1/2,1/2);(1/2,-1/2)\|}$	=	$\mathcal{O}_{\|(1/2,-1/2);(1/2,1/2)\rangle}$
$\bar{\mathcal{O}}_{\langle (1/2,-1/2);(1/2,1/2)\|}$	=	$\mathcal{O}_{\|(1/2,1/2);(1/2,-1/2)\rangle}$

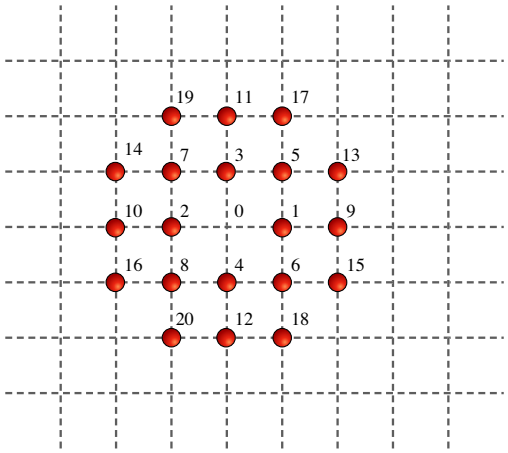

FIG. 2. Arrangement of local sources of red worldlines we used to create a source in the (j, j) representation. The site labeled 0 is the origin and is left empty. Depending on j the sources are placed on the sites marked $k = 1, 2 \ldots 2j$. The first 20 sites used in our calculations up to $j = 10$ are shown.

sites chosen for both source and sink are the same spatial sites on the $\tau = 0, L/2$ time slice. These sources and sinks can be used to compute the correlation function $C_{j,j} = \langle \bar{\mathcal{O}}_{\langle (j,j);(j,j)|} \mathcal{O}_{|(j,j);(j,j)\rangle} \rangle$, and in order to obtain $D(j, j)$ one can use the relation $C_{j,j} \sim A_{j,j} L^{-2D(j,j)}$ for large values of L. In the actual worm algorithm, one in fact computes the ratio $R_j = C_{j,j}/C_{j-1,j-1}$ and fits it to the form $(A_{j,j}/A_{j-1,j-1}) L^{-2\Delta_j}$ to compute $\Delta_j = D(j, j) - D(j-1, j-1)$ for each value of j. From these differences and setting $D(0, 0) = 1$ one can compute $D(j, j)$. Our results from [21] are tabulated in Table III for reference.

IV. SUBLEADING SECTOR

In this work we extend our earlier results in the leading sector and compute the conformal dimensions of the subleading sector, $D(j, j-1)$ for $j \geq 1$. For this we need to construct source and sink operators that transform in the representation $(j, j-1)$. We know we can construct the state $|j, j; j-1, j-1\rangle$ by applying the lowering operator J_R^- to the $|j, j; j, j\rangle$ and then constructing orthogonal states in the tensor product space. This procedure naturally leads to $2j-1$ orthonormal states, which we can label with an additional index $M = 1, 2 \ldots, (2j-1)$. Translating this to the construction of sources, we now introduce the source $\mathcal{O}_\ell = \mathcal{R}_1 \mathcal{R}_2 \ldots \mathcal{G}_\ell \ldots \mathcal{R}_{2j}$ where the red source on one lattice site ℓ is replaced by a green source where $\ell = 1, 2 \ldots, 2j$. Similarly, we introduce the corresponding sinks as $\bar{\mathcal{O}}_\ell = \bar{\mathcal{R}}_1 \bar{\mathcal{R}}_2 \ldots \bar{\mathcal{G}}_\ell \ldots \bar{\mathcal{R}}_{2j}$. We can then argue that

$$\mathcal{O}_{|(j,j);(j,j-1)\rangle} = \frac{1}{\sqrt{2j}} \sum_{\ell=1}^{2j} \mathcal{O}_\ell, \tag{6}$$

where the right-hand side is a sum over the $2j$ source terms we introduced above. Note that there are $2j-1$ sources orthogonal to Eq. (6), which we can label with $M = 1, 2 \ldots, 2j-1$ as before. These will naturally transform in the $(j, j-1)$ representation. Explicitly these sources are given by

$$\mathcal{O}^M_{|(j,j);(j-1,j-1)\rangle} = \frac{1}{\sqrt{2j}} \sum_{\ell=1}^{2j} e^{i2\pi(\ell-1)M/(2j)} \mathcal{O}_\ell. \tag{7}$$

We can similarly define the corresponding $2j-1$ sinks as

$$\bar{\mathcal{O}}^M_{\langle (j,j);(j-1,j-1)|} = \frac{1}{\sqrt{2j}} \sum_{\ell=1}^{2j} e^{-i2\pi(\ell-1)M/(2j)} \bar{\mathcal{O}}_\ell. \tag{8}$$

Since all $2j-1$ sources and sinks transform under the same irreducible representation $(j, j-1)$, any combination of them can be used in Eq. (5) to extract $D(j, j-1)$. Let us define the correlation matrix

$$C^{MM'}_{j,j-1} = \langle \bar{\mathcal{O}}^M_{\langle (j,j);(j-1,j-1)|} \mathcal{O}^{M'}_{|(j,j);(j-1,j-1)\rangle} \rangle \tag{9}$$

where we expect $C^{MM'}_{j,j-1} \sim A^{MM'}_{j,j-1} L^{-2D(j,j-1)}$ for large values of L. Practically it is more convenient to compute the average of the trace of this correlation matrix, which can be simplified to the form

$$C_{j,j-1} = \sum_\ell \left\{ \frac{1}{2j} \langle \bar{\mathcal{O}}_\ell \mathcal{O}_\ell \rangle - \frac{1}{2j(2j-1)} \sum_{\ell' \neq \ell} \langle \bar{\mathcal{O}}_\ell \mathcal{O}_{\ell'} \rangle \right\}. \tag{10}$$

Note that we also expect $C_{j,j-1} \sim A_{j,j-1} L^{-2D(j,j-1)}$.

As in the leading sector, in the worldline algorithm it is much easier to compute the ratio $\tilde{R}_j = C_{j,j-1}/C_{j,j}$. For this one constructs a worldline Monte Carlo method to generate configurations with $2j$ red sources and sinks that contribute to $C_{j,j}$. In every configuration of this ensemble, we then imagine flipping each of the $2j$ sources located at the sites $\ell = 1, 2 \ldots, 2j$ to a green source. The worldline of the green source then naturally travels through the lattice to a sink at some location ℓ'. Then we compute the contribution to $\tilde{R}_j$ from that configuration using Eq. (10), which means we add $1/2j$ if $\ell = \ell'$, or subtract the value $1/(2j(2j-1))$ if $\ell \neq \ell'$ for every value of ℓ. Averaging this contribution over the

TABLE III. Results for the conformal dimensions $D(j, j)$ up to $j = 5$ computed using worldline Monte Carlo methods in [21].

j	$D(j, j)$	j	$D(j, j)$
1/2	0.515(3)	1	1.185(4)
3/2	1.989(5)	2	2.915(6)
5/2	3.945(6)	3	5.069(7)
7/2	6.284(8)	4	7.575(9)
9/2	8.949(10)	5	10.386(11)

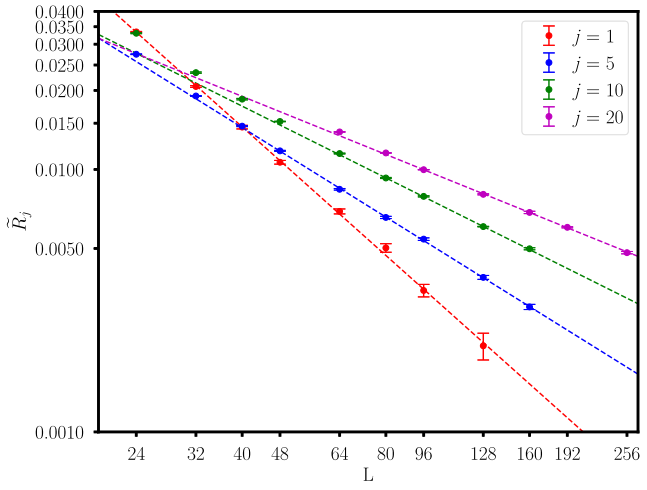

FIG. 3. Worldline Monte Carlo results for the ratio $\tilde{R}_j$ as a function of L for various values of j. The solid lines show the fits given in Table IV.

ensemble of configurations generated by the worldline algorithm gives us the ratio $\tilde{R}_j$, which is expected to scale as $(A_j/A_{j-1})L^{-2\tilde{\Delta}_j}$ where $\tilde{\Delta}_j = D(j, j-1) - D(j, j)$. Using the values of $D(j, j)$ we compute $D(j, j-1)$.

V. RESULTS

We have performed a series of Monte Carlo calculations for $1 \le j \le 10$ in increments of $1/2$, and for $j = 20$. For runs till $j = 10$, the lattice sizes ranged from $L = 32$ up to $L = 160$. At $j = 20$ we have extended our calculations up to lattice sizes of $L = 256$. For each value of j we always found that our data fit well to the expected form $C_{j,j-1}/C_{j,j} \sim L^{-2\tilde{\Delta}_j}$ for sufficiently large values of L. As examples, fits for $j = 1$, 5, 10, and 20 are illustrated in Fig. 3. From the figure, we observe that as j increases, the range of lattice sizes where a simple power law emerges changes to larger L values. The details of our fits are tabulated in Table IV.

Having obtained the values of $\tilde{\Delta}_j$ for various values of j, we try to extract the coefficients λ_i's in Eq. (2), assuming that we can neglect $\mathcal{O}(1/j^2)$ terms in the range of j values we have studied. We try several fits, as shown in Table V, to understand if the purely quantum terms λ_0 and λ_1 vanish or not. First, we note that our data for the entire range of j values fit well to the form Eq. (2), if we assume all four coefficients are nonzero (first row in Table V). On the other hand, if we drop both quantum terms the fit becomes quite bad (second row in Table V) suggesting that the quantum terms are important. In fact, the presence of any one of the two quantum terms is sufficient to bring down the χ^2/DOF considerably. For example, setting $\lambda_1 = 0$, we can get an excellent fit if we just drop the $j = 1$ data (fifth row in Table V). On the other hand, setting $\lambda = 0$ and dropping both $j = 1$, 1.5 makes the fit acceptable (sixth row in Table V). If we drop both quantum terms (i.e., set $\lambda_0 = \lambda_1 = 0$) we can only get a good fit in the range $j = 8$–20. In fact, this fit (shown as a dotted line in Fig. 4), seems unreliable as the curve deviates significantly for $j < 8$. For comparison the other good fits are also shown in Fig. 4.

Our fits clearly imply that dropping both quantum terms is not a good approximation unless the form of our fits [i.e., Eq. (2) without the quantum terms] is only valid beyond the

TABLE IV. Results of the fit of $\tilde{R}_j$ shown in Fig. 3 to the form $(A_j/A_{j-1})L^{-2\tilde{\Delta}_j}$. The range of L values used in the fit is given in the second column. We observe that as j increases this range needs to involve larger lattice sizes for a good fit.

j	L-range	$A_{j,j-1}/A_{j,j}$	$\tilde{\Delta}(j)$	χ^2/DOF
1	24–128	5.87(25)	0.813(6)	1.11
3/2	24–128	2.50(11)	0.750(6)	0.62
2	24–96	2.13(06)	0.722(4)	0.26
5/2	32–96	1.75(08)	0.685(6)	1.28
3	32–96	1.54(08)	0.659(7)	0.93
7/2	32–96	1.35(05)	0.633(5)	0.38
4	32–96	1.18(04)	0.607(4)	0.40
9/2	40–160	1.05(04)	0.586(5)	0.94
5	40–160	0.94(04)	0.566(5)	0.89
11/2	48–160	0.90(03)	0.555(4)	0.66
6	48–160	0.83(03)	0.541(5)	1.40
13/2	64–160	0.75(04)	0.525(7)	1.11
7	64–160	0.71(03)	0.513(5)	1.18
15/2	64–160	0.69(04)	0.506(6)	1.45
8	64–160	0.60(03)	0.486(5)	0.77
17/2	64–160	0.61(03)	0.484(5)	0.83
9	80–160	0.53(04)	0.467(8)	0.98
19/2	80–160	0.53(03)	0.463(7)	0.47
10	80–160	0.50(02)	0.454(5)	0.63
20	96–256	0.28(01)	0.367(3)	0.65

TABLE V. Fits of $\tilde{\Delta}_j$ to the functional form given in Eq. (2). We first consider the whole range of j in the first four rows. While including all four coefficients as fitting parameters gives an excellent fit, setting the two purely quantum mechanical terms $\lambda_0 = \lambda_1 = 0$ makes the fit quite bad. Including even one of them is sufficient to improve the fit considerably. Setting two of the fitting parameters to zero is only possible by shrinking the allowed region of j considerably, which we believe makes the fitting procedure unreliable.

j range	λ_0	$\lambda_{1/2}$	λ_1	$\lambda_{3/2}$	χ^2/DOF
1–20	0.07(2)	1.5(1)	−1.0(2)	0.3(1)	0.6
1–20	0	1.42(1)	0	−0.69(1)	48
1–20	0	1.96(2)	−1.83(6)	0.69(5)	1.8
1–20	0.16(1)	0.98(2)	0	−0.34(2)	2.3
1.5–20	0.13(1)	1.07(2)	0	−0.47(3)	0.3
2–20	0	2.06(3)	−2.27(14)	1.14(13)	1.1
8–20	0	1.81(2)	0	−3.5(2)	1.1
8–20	0	2.09(4)	−2.02(13)	0	0.6

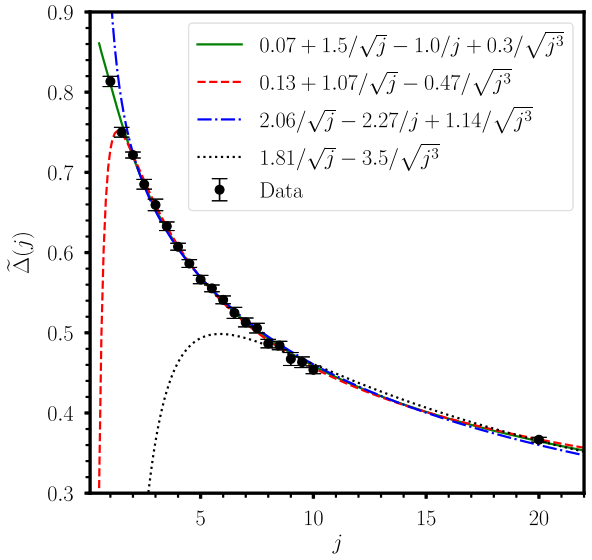

FIG. 4. Plot of $\tilde{\Delta}_j$ as a function of j from Table IV. The lines shown are fits to the form given in Eq. (2) with parameter values given in the first (solid), fifth (dashed), sixth (dashed-dotted), and seventh (dotted) rows of Table V.

range of j's studied here. On the other hand, our data are consistent with the conjecture that $\lambda_0 = 0$, if we allow for $\lambda_1 \neq 0$ (see the dot-dashed line in Fig. 4, which only deviates at $j = 1, 1.5$). Unfortunately we cannot rule out $\lambda_0 \neq 0$, but our results show that it is small, if at all present.

VI. CONCLUSIONS

In this work we have constructed a Monte Carlo method to compute the subleading conformal dimensions in the large charge expansion at the $O(4)$ Wilson-Fisher fixed point. We used this method to compute $\tilde{\Delta}_j$ for several values of j in the range $1 \leq j \leq 20$. While our results are consistent with the general predictions of the expansion given in Eq. (2), we cannot rule out the possibility that $\tilde{\Delta}_j$ approaches a nonzero constant λ_0 in the large j limit. However, our data are consistent with the conjecture in the literature (see Ref. [22]) that $\lambda_0 = 0$, but then we need $\lambda_1 \neq 0$. Assuming this to be true, we can estimate the three leading terms in the expansion to be $\lambda_{1/2} \approx 2.1(1)$, $\lambda_1 \approx 2.3(2)$, and $\lambda_{3/2} \approx 1.2(2)$. We hope our work will motivate a better analytic understanding of the purely quantum terms λ_0 and λ_1. This could guide Monte Carlo calculations for $j \gg 20$, which require much larger computational resources.

ACKNOWLEDGMENTS

We thank D. Orlando and S. Reffert for extensive discussions and collaborating with us in the past. We also thank S. Hellerman for useful discussions about this work. The material presented here is based upon work supported by the U.S. Department of Energy, Office of Science, Nuclear Physics program under Award No. DE-FG02-05ER41368.

[1] S. Rychkov, *EPFL Lectures on Conformal Field Theory in D>=3 Dimensions*, Springer Briefs in Physics (Springer, New York, 2016), 10.1007/978-3-319-43626-5.
[2] D. Simmons-Duffin, in *Theoretical Advanced Study Institute in Elementary Particle Physics: New Frontiers in Fields and Strings* (World Scientific, Singapore, 2017), pp. 1–74, 10.1142/9789813149441_0001.
[3] Z. Komargodski and A. Zhiboedov, J. High Energy Phys. 11 (2013) 140.
[4] S. Hellerman, D. Orlando, S. Reffert, and M. Watanabe, J. High Energy Phys. 12 (**2015**) 071.
[5] A. Kaviraj, K. Sen, and A. Sinha, J. High Energy Phys. 11 (2015) 083.
[6] A. Kaviraj, K. Sen, and A. Sinha, J. High Energy Phys. 07 (2015) 026.
[7] L. F. Alday, Phys. Rev. Lett. **119**, 111601 (2017).
[8] R. Gopakumar, A. Kaviraj, K. Sen, and A. Sinha, Phys. Rev. Lett. **118**, 081601 (2017).
[9] P. Dey, K. Ghosh, and A. Sinha, J. High Energy Phys. 01 (2018) 152.
[10] S. Caron-Huot, J. High Energy Phys. 09 (2017) 078.
[11] S. Hellerman and S. Maeda, J. High Energy Phys. 12 (2017) 135.
[12] S. Hellerman, S. Maeda, and M. Watanabe, J. High Energy Phys. 10 (2017) 089.
[13] D. Jafferis, B. Mukhametzhanov, and A. Zhiboedov, J. High Energy Phys. 05 (2018) 043.
[14] L. Alvarez-Gaume, D. Orlando, and S. Reffert, J. High Energy Phys. 12 (2019) 142.
[15] D. Orlando, S. Reffert, and F. Sannino, Phys. Rev. D **101**, 065018 (2020).
[16] D. Poland, S. Rychkov, and A. Vichi, Rev. Mod. Phys. **91**, 015002 (2019).
[17] N. Dondi, I. Kalogerakis, D. Orlando, and S. Reffert, J. High Energy Phys. 05 (2021) 035.
[18] A. Monin, Phys. Rev. D **94**, 085013 (2016).
[19] A. de la Fuente, J. High Energy Phys. 08 (2018) 041.
[20] D. Banerjee, S. Chandrasekharan, and D. Orlando, Phys. Rev. Lett. **120**, 061603 (2018).
[21] D. Banerjee, S. Chandrasekharan, D. Orlando, and S. Reffert, Phys. Rev. Lett. **123**, 051603 (2019).
[22] L. A. Gaumé, D. Orlando, and S. Reffert, Phys. Rep. **933**, 2180 (2021).
[23] We thank D. Orlando for pointing this out to us and helping us understand the discussion presented in this paragraph.

[24] L. Alvarez-Gaume, O. Loukas, D. Orlando, and S. Reffert, J. High Energy Phys. 04 (2017) 059.
[25] S. Hellerman, N. Kobayashi, S. Maeda, and M. Watanabe, J. High Energy Phys. 10 (**2019**) 038.
[26] O. Antipin, J. Bersini, F. Sannino, Z.-W. Wang, and C. Zhang, Phys. Rev. D **102**, 045011 (2020).
[27] In Ref. [21] it was predicted that $\lambda_0 \neq 0$, based on an incorrect assumption. This error was later corrected in Ref. [22].
[28] D. Cecile and S. Chandrasekharan, Phys. Rev. D **77**, 014506 (2008).
[29] H. Singh and S. Chandrasekharan, Phys. Rev. D **100**, 054505 (2019).
[30] H. Singh, arXiv:1911.12353.
[31] T. Bhattacharya, A. J. Buser, S. Chandrasekharan, R. Gupta, and H. Singh, Phys. Rev. Lett. **126**, 172001 (2021).